

On properties of seawater, defined by temperature, salinity and pressure

By George Veronis
Journal of Marine Research 30(2):227–255
1972

This document may be used for personal, research and educational purposes, including presentations, academic and classroom materials, nonprofit publications, and nonprofit websites, as long as attribution to the original source is included in the use.

For any commercial use contact
the *Journal of Marine Research* Editorial Office for information.

© 1972 George Veronis



On Properties of Seawater Defined by Temperature, Salinity, and Pressure¹

George Veronis

*Geology and Geophysics
Yale University
New Haven, Connecticut 06520*

ABSTRACT

Hydrographic station data, consisting principally of temperature and salinity determinations, have been used by physical oceanographers to develop a climatological picture of the distribution of these quantities in the oceans of the world. Density as determined by Knudsen's formula, taken together with hydrostatic and geostrophic dynamics, also provides a crude picture of oceanic flow. However, the data probably contain substantially more information than has been derived from them in the past.

The quantity that is orthogonal to potential-density curves in the θS plane is suggested as a useful variable to complement the information contained in potential density. The derivation of this quantity, denoted by τ in this paper, is straightforward. A polynomial expression for τ that is suitable for computer calculations of τ from hydrographic station data is given. Shown are examples of hydrographic station data from the Atlantic plotted on the $\tau\sigma_\theta$ diagram. The information contained in the $\tau\sigma_\theta$ diagram shows many of the features exhibited in the TS plane. Vertical sections of τ appear to provide information about mixing in different parts of the Atlantic. The distribution of τ for abyssal waters at selected stations in the oceans of the world resembles the distribution of abyssal density as plotted by Lynn and Reid (1968). From the data presented, it appears that τ may serve as a good tracer for abyssal water movements.

Since τ is defined to be orthogonal to σ_θ , the expectation is that τ is a dynamically passive variable. However, since σ_θ does not correlate with abyssal densities, it appears to lose dynamical significance at great depth, and τ assumes dynamical significance because of its orthogonality to σ_θ . This unexpected feature leads to an exploration of the dynamical significance of σ_θ . A natural starting point is the question of stability of abyssal water.

A distinction is made between stability as determined by in situ determinations and as determined by the potential-density (σ_θ) distribution. Simple examples are presented to show that analysis based on σ_θ alone can lead to incorrect conclusions about gravitational stability of the water in the abyssal ocean. The reason is that seawater is a multicomponent thermodynamic system, and the thermodynamic coefficients are functions of pressure, salinity, and temperature. This functional dependence leads to adjustments in density as a water particle moves adiabatically in the vertical direction so that a layer of water that appears to be unstable near the surface may be stable (as determined by in situ determination) at great depth.

1. Accepted for publication and submitted to press 23 February 1972.

A local potential density, which is simply the vertical integral of the in situ stability, is derived. This quantity gives a precise picture of gravitational stability in the vertical direction. Some distributions of local potential density are shown.

1. *Introduction.* The many temperature (T) and salinity (S) measurements obtained by oceanographers during the past century have enabled us to form a climatological picture of the oceans. On oceanographic cruises, these data are the most frequently gathered, and they form the largest single source of information about large-scale flow in the ocean. The usefulness of temperature and salinity data is significantly enhanced by the use of the TS diagram (Helland-Hansen 1916) on which characteristic features of the TS distribution can be seen. Knudsen's (1901) formula for determining the density from given values of T and S , taken together with the geostrophic and hydrostatic approximations, provides a zero-order picture of the dynamics of ocean currents. Yet it is very likely that the data contain considerably more information than has been obtained from them up to the present time. In this paper an approach is presented that is an alternative, and hopefully a useful supplement, to classical water-mass analysis.

As a starting point for this study, a brief outline of density functions is helpful. Density (ρ) can be determined from known values of temperature, salinity, and pressure (p). In oceanography, it is customary to use sigma (σ), defined as 1000 times the difference between the in situ density² and the density of pure water (in cgs units) at 4°C and atmospheric pressure:

$$\sigma(T, S, p) = 1000 [\rho(T, S, p) - 1 \text{ g/cm}^3].$$

The most commonly used density variable is sigma-t, defined as

$$\sigma_t(T, S) = \sigma(T, S, 0),$$

where the direct effect of pressure on density is absent, and water from all levels can be compared. For dynamical³ purposes it is preferable to use the potential density, σ_θ , which is defined as σ_t but with the potential temperature, θ , replacing T :

$$\sigma_\theta = \sigma_t(\theta, S).$$

The preference for σ_θ lies in the fact that the pressure effect on temperature is removed when θ replaces T and σ_θ is a true measure of the potential

2. Strictly speaking, oceanographic determinations are based on specific gravity; but since the reference is distilled water at 4°C, the density and specific gravity are nearly identical numerically when cgs units are used.

3. The term "dynamical" is used here in the strict sense of physics and *not* as it is conventionally used in oceanography, e.g., as in "dynamical" computations. A parcel of seawater is assumed to make an adiabatic adjustment when it undergoes a change of pressure and the properties of the parcel, after such an adjustment, are taken to be the properties that are important or significant for the dynamical interaction of that parcel with its surroundings.

density. The widespread use of σ_t rather than σ_θ is unfortunate. In near-surface waters the temperature variation is large, and, since σ_t and σ_θ differ only slightly, either can be used to give an adequate description of the dynamically significant density distribution. In deeper water, however, the differences between σ_t and σ_θ are relatively significant, and the use of σ_θ is distinctly preferable. In more recent studies of distributions of quantities in deep water (e.g., Lynn and Reid 1968, Worthington and Wright 1970) the tendency has been to use σ_θ .

Since the potential density is defined to contain the dynamically significant part of the temperature and salinity distributions, it is often desirable to look at distributions (say, vertical sections or isopleths at a given level) of σ_θ , even though σ_θ is a derived rather than an observed quantity. Now, how is one to supplement the σ_θ graph? With graphs of salinity? With graphs of potential temperature? It is clear from the derivation of σ_θ that some portion of θ and S is implicit in each value of σ_θ , so that displaying either θ or S in concert with σ_θ will yield some redundant information. Displaying *both* θ and S as well as σ_θ would increase the redundancy, but it would still not be clear which part of the θ and S distributions is included in σ_θ . Hence, one is led to the question: Is there a variable that can supplement σ_θ and that contains temperature and salinity information not included in σ_θ ?

The answer to this question is obvious. The variable must have isopleths in the θS plane that are orthogonal to the isopleths of σ_θ . Contours of such a variable, denoted by $\tau = \text{const}$, are shown in Fig. 1. It is evident that τ undergoes a maximum change along a curve for which $\sigma_\theta = \text{const}$ and that τ remains constant along the normal gradient direction of σ_θ . Hence, it is the most efficient variable that one can use to supplement the information contained in σ_θ . Since it is orthogonal to σ_θ in the θS plane, it is conservative during an adiabatic change, as is σ_θ .

There are several points to be made in connection with the variable, τ . The first and most obvious is that τ is not unique. The definition depends on the chosen scales of S and θ . In Fig. 1, the θS plane is the one used by the Chesapeake Bay Institute with 0.05 inch corresponding to increments of $\Delta S = 0.02\text{‰}$ and $\Delta T = 0.1^\circ\text{C}$. Near $\theta = 9.42^\circ\text{C}$ and $S = 35\text{‰}$, an increment of $\Delta S = 0.02\text{‰}$ gives a change in σ_θ that is nearly the same as that produced by an increment of $\Delta T = 0.1^\circ\text{C}$. The second point is that, unlike temperature or salinity, τ cannot be measured. It owes its existence to abstract reasoning.⁴ The only physical interpretation that can be given to it is that it contains that combination of θ (or T) and S that does not affect σ_θ (or σ_t). As such, it may serve a useful purpose as a tracer or as a measure of mixing along σ_θ surfaces.

4. The only other reference to τ that I have seen is in an interesting short paper by Stommel (1962), who attempts to show that the TS relationship characteristic of abyssal water may be a dynamical consequence of the distribution of τ (called q in his paper). I have asked a variety of physical chemists, solution chemists, chemical engineers, and geochemists if they were familiar with τ , but I have invariably drawn a blank.

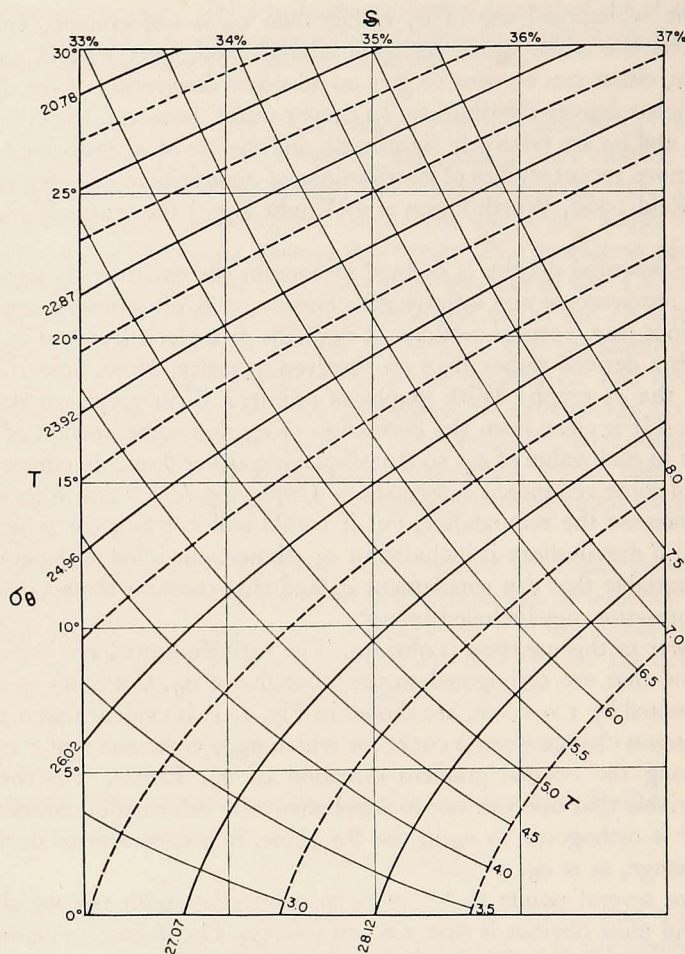


Figure 1. Curves of $\tau = \text{const}$ slope upward to the left and are orthogonal to the $\sigma_\theta = \text{const}$ curves. Values of σ_θ and τ along the respective curves are shown at the ends of the curves. The basic figure is a reproduction of the TS diagram produced by the Chesapeake Bay Institute. The $\sigma_\theta = \text{const}$ curves are normally given in terms of thermosteric anomaly in cl/ton.

The derivation of τ is given in § 2. Also contained there is a polynomial expression for τ , where the coefficients are determined by minimizing the mean-square error that the polynomial yields when compared with the derived values for τ . The polynomial is suitable for computer calculations.

§ 3 includes several distributions of τ . In Figs. 2-4, profiles of τ for stations in the western South Atlantic, the eastern North Atlantic, and the northern Mediterranean show how τ is distributed in the vertical plane. Some of the more striking features of the salinity profiles are mirrored in the τ profiles.

In Figs. 5 and 6, diagrams of θ vs S are shown for stations in the North and South Atlantic where some well-known characteristic features are present. Corresponding diagrams of τ vs σ_θ are given in Figs. 7 and 8, and the analogous features are discussed. The advantage of the $\tau\sigma_\theta$ diagram is that it exhibits certain dynamical features more readily than does a θS diagram.

Fig. 9 shows a vertical section of τ along 36°N in the Atlantic Ocean and indicates the influence of Mediterranean outflow east of the Mid-Atlantic Ridge. West of this Ridge the presence of Mediterranean water is indicated by the intersection of σ_θ (shown by dashes) and τ contours at a level of about 1300 m. A vertical section of τ (Fig. 10) in the western North Atlantic together with the corresponding section of σ_θ indicates substantial mixing of waters below 1000 m depth throughout the latitudinal range (60°S to 40°N). Abyssal values of τ for the world oceans are shown in Fig. 15 at the same stations for which Lynn and Reid (1968) have presented values of σ_θ , θ , and S . Lynn and Reid have pointed out that at great depths the distribution of σ_θ does not correlate well with any of the other variables. However, they have shown that the potential density referred to the 4000-m level (σ_4) correlates much better with potential temperature and exhibits features that make it useful as a tracer. The distribution of τ possesses the same desirable features, hence, it may serve as a very useful indicator of abyssal water movement.

The good correlation of τ with σ_4 , taken together with the poor $\sigma_\theta - \sigma_4$ correlation, indicates that in deep waters potential density may not be dynamically significant. This point is pursued in §§ 4 and 5, where it is shown that, even though σ_θ is defined precisely and unambiguously, it cannot be used indiscriminately. For example, in determining the gravitational stability⁵ of deep water, one cannot generally use σ_θ . The reason is that seawater is a multi-component fluid, and waters of different salinities and temperatures have different values of the thermodynamic coefficients (thermal expansion, compressibility, etc.). Small but significant differences in the dynamically significant part of the densities of different parcels of fluid can be masked by the changes brought about by the calculation of potential density, and erroneous interpretation can result. This point has been recognized by some workers (Wüst 1933, Schubert 1935, Kawai 1966, Lynn and Reid 1968), but it has not been generally appreciated nor have the reasons for the apparently paradoxical results been fully understood. Two examples of the paradox together with a discussion of the associated problems are presented in § 4.

Gravitational stability based on potential-density distribution is associated with a finite, vertical, adiabatic displacement of water parcels. The classically accepted gravitational stability of ocean waters (Hesselberg and Sverdrup 1914)

5. In a single-component system, potential density is completely determined by potential temperature, and either one can be used to determine the gravitational stability of the system. One might *hope* that in a multicomponent system potential density would serve the same purpose because the pressure effect on density is removed. In theoretical analyses, in which the Boussinesq approximation is used, there is a tacit assumption that potential density does determine the gravitational stability of the fluid.

is based on an infinitesimal vertical displacement of parcels. There is a fundamental difference between these two approaches to stability. If the system is disturbed by small-amplitude fluctuations, the Hesselberg-Sverdrup criterion is applicable. However, if some process were to displace a layer of water a finite distance in the vertical plane (the displacement could involve a large horizontal distance as well), then stability determined by potential density becomes meaningful. This point is discussed in § 5, where a "new" density distribution in the vertical plane is introduced. This density—called local potential density and denoted by ρ_l —is obtained by calculating the in situ gravitational stability, *a la* Hesselberg and Sverdrup, and then integrating this derivative of the density from the surface downward. The distribution so obtained is meaningful only in the vertical direction, but it affords an instantaneous picture of the infinitesimal gravitational stability of each column of water. Examples are presented for individual stations in the Mediterranean and the Atlantic. Comparison of the local potential density with σ_θ in the different regions is instructive. When the water is fairly homogeneous in θ and S , as it is in the northwestern Mediterranean during the winter, the local potential density gives the same information as σ_θ . However, for typical stations in the Atlantic, the two variables differ substantially. In this case σ_θ cannot be used as a measure of gravitational stability—at least not in the sense of indicating vertical overturning. However, σ_l [$\equiv 1000(\rho_l - 1)$] is defined to give just such a picture. The accuracy of the determination of σ_l is limited by the truncation error associated with vertical spacing of samples at individual stations.

Vertical profiles of σ_l for data from the Atlantic show that in deep water σ_l correlates well with τ but not at all with σ_θ . It has already been pointed out that horizontal abyssal distributions show that potential density referred to 4000 m correlates with τ but not with σ_θ . Hence, in deep water, τ correlates better with variables that are known to be dynamically significant than does σ_θ .

2. *Derivation of τ .* The potential density (or σ_t) curves in the θS (or TS) plane are curves along which σ_θ (or σ_t) is constant. It was noted in § 1 that the information contained in σ_θ can be supplemented most efficiently by that variable whose curves in the θS plane are orthogonal to the curves $\sigma_\theta = \text{const}$. The derivation of this orthogonal variable is outlined here.

The differential form for σ_θ (θ, S) is

$$d\sigma_\theta = \frac{\partial \sigma_\theta}{\partial S} dS + \frac{\partial \sigma_\theta}{\partial \theta} d\theta. \quad (1)$$

Hence, the slope of the curves $\sigma_\theta = \text{const}$ in the θS plane is

$$\frac{d\theta}{dS} = - \frac{\partial \sigma_\theta / \partial S}{\partial \sigma_\theta / \partial \theta}. \quad (2)$$

Denote the curves orthogonal to $\sigma_\theta = \text{const}$ by $\tau = \text{const}$. Then the differential expression for these curves is

$$d\tau = \frac{\partial \tau}{\partial S} dS + \frac{\partial \tau}{\partial \theta} d\theta, \quad (3)$$

and

$$\frac{d\theta}{dS} = - \frac{\partial \tau / \partial S}{\partial \tau / \partial \theta} \quad (4)$$

along $\tau = \text{const}$.

Since the curves $\tau = \text{const}$ are orthogonal to the curves $\sigma_\theta = \text{const}$, the *non-dimensional* slope corresponding to (2) must be the negative reciprocal of the nondimensional slope corresponding to (4). Hence

$$\frac{\partial \tau / \partial S \Delta S}{\partial \tau / \partial \theta \Delta \theta} = - \frac{\partial \sigma_\theta / \partial \theta \Delta \theta}{\partial \sigma_\theta / \partial S \Delta S}, \quad (5)$$

where ΔS and $\Delta \theta$ are convenient scaling factors for rendering the slopes non-dimensional. The particular values of ΔS and $\Delta \theta$ will depend on the respective scales in the graph that is used. Now, since σ_θ is a known function of θ and S (by Knudsen's formula), (5) is the differential equation for the curves $\tau = \text{const}$.

Eq. (5) can be satisfied formally by writing

$$\frac{\partial \tau}{\partial S} = -a(\theta, S) \frac{\partial \sigma_\theta \Delta \theta}{\partial \theta \Delta S}, \quad \frac{\partial \tau}{\partial \theta} = a(\theta, S) \frac{\partial \sigma_\theta \Delta S}{\partial S \Delta \theta}, \quad (6)$$

where $a(\theta, S)$ is an arbitrary function of θ and S . For present purposes⁶ it suffices to take $a = \text{const}$ and to rescale τ as τ/a .

Substituting (6) into (3) yields (with $d\tau$ now corresponding to $d\tau/a$)

$$d\tau = - \frac{\partial \sigma_\theta \Delta \theta}{\partial \theta \Delta S} dS + \frac{\partial \sigma_\theta \Delta S}{\partial S \Delta \theta} d\theta. \quad (7)$$

Now choose the increments dS and $d\theta$ along a curve $\sigma_\theta = \text{const}$. Then substituting the value for $d\theta$ from (2) into (7) yields

$$d\tau = - \left[\frac{\partial \sigma_\theta \Delta \theta}{\partial \theta \Delta S} + \frac{(\partial \sigma_\theta / \partial S)^2 \Delta S}{\partial \sigma_\theta / \partial \theta \Delta \theta} \right] dS, \quad (8)$$

and solving (8) for dS yields

6. This argument produces a straightforward determination of τ . However, since the numerical derivation of τ depends on the scales that are chosen, the present method gives only one such determination. It may be that a definition not coupled to a specific choice of scales (as in the present one) may be preferable. This point was made to me by N. P. Fofonoff (private communication).

$$dS = - \left(\frac{\partial \sigma_\theta}{\partial \theta} \right) d\tau / \left[\frac{\Delta \theta}{\Delta S} \left(\frac{\partial \sigma_\theta}{\partial \theta} \right)^2 + \frac{\Delta S}{\Delta \theta} \left(\frac{\partial \sigma_\theta}{\partial S} \right)^2 \right]. \quad (9)$$

In a numerical procedure, one can choose a convenient value of τ at some suitable point in the θS plane; then, for given increments $\delta\tau$ along the curve $\sigma_\theta = \text{const}$ through that point, one can use (9) to evaluate corresponding increments δS . The finite difference form of (2) then yields $\delta\theta$. Finally, starting at points on the chosen $\sigma_\theta = \text{const}$ curve, on which values of τ have already been calculated, one can construct the orthogonal trajectories to the $\sigma_\theta = \text{const}$ curve by using (4) and (5). These orthogonal trajectories are curves of constant τ .

The foregoing procedure was followed and τ was calculated for the ranges $0 \leq \theta \leq 30^\circ\text{C}$, $33\text{‰} \leq S \leq 37\text{‰}$. If the θS diagram of the Chesapeake Bay Institute is used, the appropriate scaling factors for nondimensionalizing the slope are $\Delta\theta = 0.1^\circ\text{C}$ and $\Delta S = 0.02\text{‰}$, since these correspond to 0.05-inch divisions on the CBI graph. In the actual numerical calculations, the arbitrary value of $\tau = 5.0$ at $\theta = 9.42^\circ\text{C}$ and $S = 35\text{‰}$ was chosen and a fine network of values of τ was calculated. A few of the curves $\tau = \text{const}$ are shown in Fig. 1. The range of τ is from approximately 2.5 to 10.0. Thus, the range is numerically comparable to that of σ_θ .

With present-day computers it is more convenient to evaluate τ from an empirical formula rather than to have to resort to a graph. Hence, a polynomial expression for τ was generated by calculating the coefficients that give a least-mean-squares fit to 100 scattered values calculated by the foregoing procedure. The polynomial is of the fifth degree in θ and S and yields values of τ that agree with the numerically calculated ones to within 0.002 units. This accuracy is better than the reliability of σ_θ (on which τ depends) from θS data and should suffice for any conceivable use of τ . The empirical formula is

$$\tau = \sum_{i=1}^6 \sum_{j=1}^6 A_{ij} \theta^{i-1} S^{j-1}, \quad (10)$$

where the values of the A_{ij} are given in Table VI.

The usefulness of τ for theoretical modeling depends on whether its distribution can be described by a mathematical expression. On the assumption that molecular diffusion of salt and heat are unimportant in large-scale models, it is possible to derive an appropriate equation.

Thus, suppose that θ and S are simply advected by the flow so that the equations

$$\frac{d\theta}{dt} = 0, \quad \frac{dS}{dt} = 0 \quad (11)$$

are valid. Since τ is a function of θ and S , it is possible to write

$$\frac{d\tau}{dt} = \frac{\partial \tau}{\partial \theta} \frac{d\theta}{dt} + \frac{\partial \tau}{\partial S} \frac{dS}{dt} \quad (12)$$

or

$$\frac{d\tau}{dt} = 0 \quad (13)$$

by use of (11).

Now separate τ and the velocity, v , into ensemble means, $\bar{\tau}$ and \bar{v} , and fluctuations about the mean, τ' and v' . Substituting such a separation into (13) and taking the ensemble mean yields

$$\frac{d\bar{\tau}}{dt} + \overline{v' \cdot \nabla \tau'} = 0$$

or

$$\frac{d\bar{\tau}}{dt} + \nabla \cdot (\overline{v' \tau'}) = 0, \quad (14)$$

where (14) is valid if the fluid is incompressible. If a coefficient of eddy diffusivity is introduced into (14) in the usual fashion, the resulting equation is

$$\frac{d\bar{\tau}}{dt} = \nabla \cdot (A \nabla \bar{\tau}). \quad (15)$$

A similar equation, with $\bar{\sigma}_\theta$ replacing $\bar{\tau}$, can be derived for σ_θ . If τ is dynamically passive, eq. (15) allows one to use $\bar{\tau}$ as a tracer. Boundary conditions on $\bar{\tau}$ can be expressed in terms of boundary conditions on θ and S .

3. *Distributions of τ .* In Figs. 2, 3, and 4 are shown vertical profiles of τ together with the corresponding profiles of S , θ , and σ_θ . In the Atlantic Ocean, τ has the range $3 \leq \tau \leq 8$, with larger values occurring near the surface and smaller values near the bottom. Vertical profiles of τ exhibit greater fluctuations than do those of σ_θ . Since σ_θ is, by definition, the dynamically significant variable, it tends to stratify monotonically. The variable τ is dynamically passive and tends to act more as a tracer. Hence, it can have a much more variable structure in the vertical plane.⁷ The minimum value of τ that occurs near 900-m depth in Fig. 3 lies below a salinity minimum. In Fig. 2 the interval of unstable salinity stratification is an interval of smaller (but monotonic) change in τ . The Mediterranean Station, in Fig. 4, shows a nearly mixed column of water, and it is difficult to draw general conclusions from the profile shown. However, since τ contains the dynamically passive components of θ and S , it may serve as a single indicator of mixing.

7. Tracers such as O_2 or Cl^{34} , which are dynamically passive, also exhibit variable structures. Even salinity, which contributes less to the stable stratification of the oceans than does temperature, can have several subsurface maxima and minima.

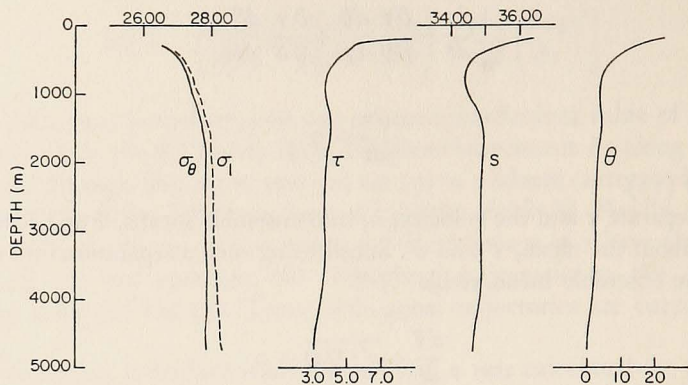


Figure 2. Vertical profiles of S , σ_θ , τ , and σ_l for CRAWFORD St. 127. The data are given in Table III.

Figs. 5 and 6 show θS diagrams of (evenly spaced) stations selected from data along 36°N in the Atlantic and along a north-south section in the western Atlantic, respectively. In Fig. 5 the influence of Mediterranean water is evident in the high-salinity values that show up as tongues in the θS diagram. This high salinity steadily decreases with longitude, with its maximum value at the 10°W station. At 60°W there is essentially no evidence of the Mediterranean water at this latitude.

In the θS diagram for the western Atlantic stations, the salinity maximum of Mediterranean water is again evident for the stations north of 8°N . Antarctic Intermediate Water shows up as a salinity minimum for the South Atlantic stations.

As an alternative one can look at the $\tau\sigma_\theta$ diagrams shown in Figs. 7 and 8

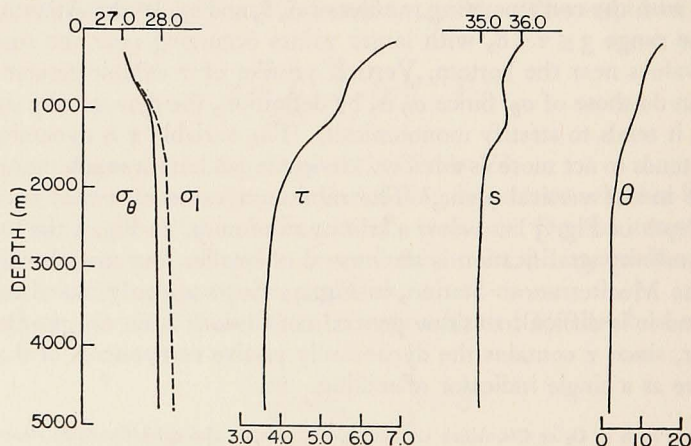


Figure 3. Vertical profiles of S , σ_θ , τ , and σ_l for CHAIN St. 63. The data are given in Table IV.

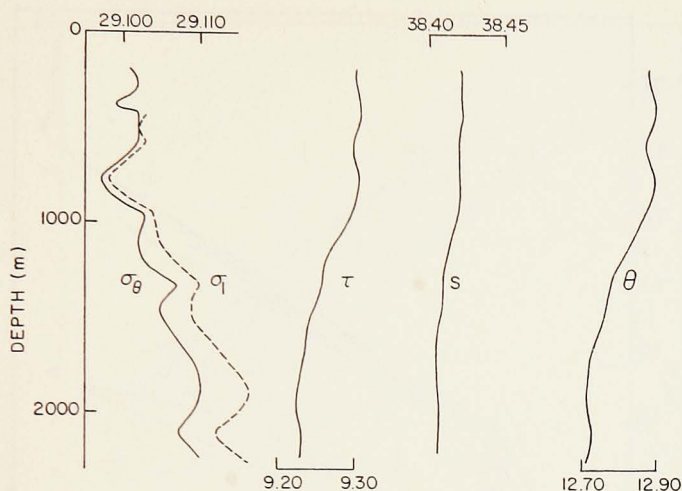


Figure 4. Vertical profiles of S , σ_θ , τ , and σ_l for DISCOVERY St. 6749. The data are given in Table V.

for the same station data. In Fig. 7, high τ values in the 36°N section are evidence of the influence of Mediterranean water. These higher values also decrease with increasing longitude, and again there is no evidence of Mediterranean influence at 60°W .

Fig. 8 shows the influence of Mediterranean water with rather larger values of τ for latitudes north of 8°N . The presence of Antarctic Intermediate Water is exhibited by the successively decreasing values of τ with latitude for the South Atlantic stations.

Individual small-scale features in the θS diagram can be identified in the $\tau\sigma_\theta$ diagram. In fact, it is possible to see the variation in τ and σ_θ from the θS diagram itself, which normally contains σ_θ curves and on which τ curves can be drawn. (If the θS diagram is rotated 45° clockwise, it resembles the $\tau\sigma_\theta$ diagram). However, for present purposes it seems best to show the $\tau\sigma_\theta$ diagram separately.

Figs. 9 and 10 show vertical sections of τ along 36°N in the North Atlantic and along a longitudinal section in the western Atlantic. Corresponding sections for σ_θ are shown in Figs. 11 and 12. In Fig. 9 one can see a blob with $\tau > 6.0$ in the eastern Atlantic. This feature indicates mixing with Mediterranean outflow that has high salinity and high values of τ (> 9.0). In Fig. 9, a few isopleths of σ_θ are superimposed as dashed curves. Where no dashed curves are drawn, contours of σ_θ and τ are more or less parallel. In such regions, θ is related to S , as can be seen by referring to the θS diagrams (Figs. 5 and 6). The fact that a θS relationship obtains when σ_θ and τ are parallel is indicated in § 6.

In order to interpret the significance of the distributions of τ , it is necessary

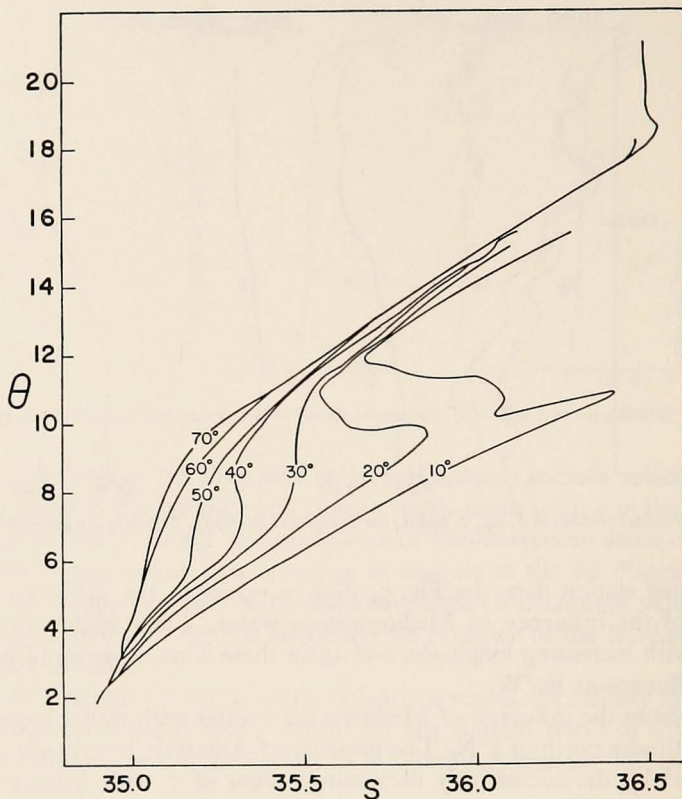


Figure 5. The θS diagram for stations along $36^{\circ}N$ in the Atlantic Ocean. The approximate longitude is marked on each curve.

to have some physical process in mind, because the same distribution can be interpreted in different ways. Suppose, for example, that τ is observed to have a constant value along a constant σ_{θ} surface. This distribution could arise if the water were formed in some surface location and if intense lateral mixing were to obliterate any τ variations along the constant σ_{θ} surface. On the other hand, if all of the water with a particular value of σ_{θ} were formed in a given location where τ was constant and if this water were simply advected with no lateral mixing, then τ would again be constant along a constant σ_{θ} surface. However, the first alternative appears to describe a more likely situation, so that regions where σ_{θ} and τ contours parallel each other will be interpreted as ones with intense horizontal mixing. (This interpretation of regions of parallel σ_{θ} and τ contours was suggested to me by R. B. Montgomery).

Consider the case where τ is observed to vary along a constant σ_{θ} surface. Such a variation could be associated with a time variation of τ at the point of origin and subsequent flow with no lateral mixing along a constant σ_{θ} surface.

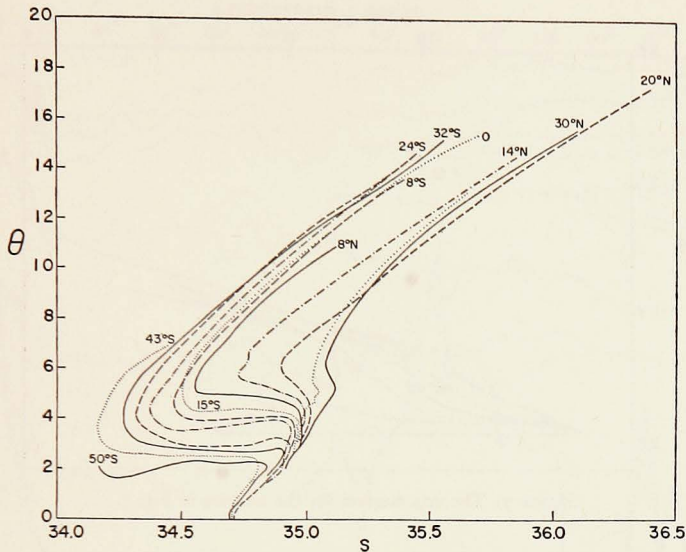


Figure 6. The θS diagram for stations along a north-south section in the western Atlantic. The approximate latitude is marked on each curve. Dashed curves etc. are used to distinguish stations.

Or it could be that the water at the point of origin has a constant τ value, with some lateral mixing with waters of different τ values on the surface where σ_θ is constant. A third possibility is that the water, as it progresses horizontally, mixes with overlying and underlying water so that the values of τ are altered. In this case it is the *vertical* mixing process that is important; lateral mixing cannot be very strong, otherwise horizontal variations would be smoothed out. In their section on water-mass analysis, Sverdrup *et al.* (1942) have chosen this last interpretation for observed horizontal differences in properties. This interpretation seems to be widely accepted and will be adopted here.

If τ can be used as a measure of mixing, then the fact that the two sets of curves intersect in the eastern basin indicates the presence of relatively strong vertical mixing but moderate or weak lateral mixing east of the Mid-Atlantic Ridge. West of this Ridge the only isopleth of σ_θ that clearly intersects the τ curves is near the 1300-m depth. This is approximately the level of the water that has mixed with water from the Mediterranean according to water-mass analysis.

The north-south section of τ in the western Atlantic (Fig. 10) shows a blob of fluid with $\tau > 4.0$ centered at about 1200 m between the equator and 10°N . The potential temperature [see Lynn and Reid (1968) for comparable north-south sections of θ and S] shows a slight increase with depth in this region, so that τ reflects this feature. This latitudinal band embraces the Equatorial Counter Current. The characteristic features normally identified as Antarctic

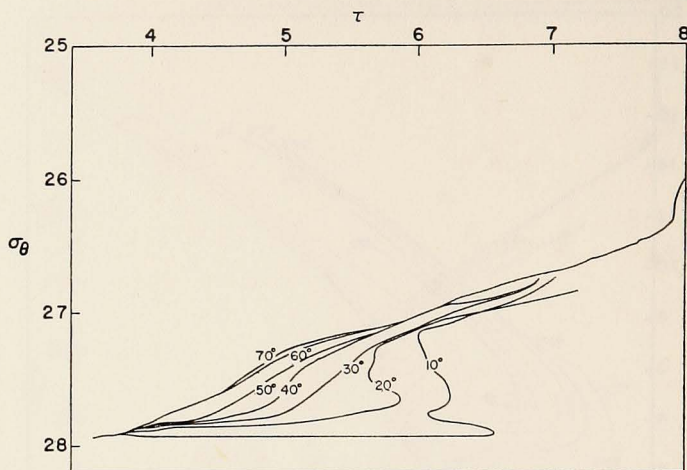


Figure 7. The $\tau\sigma_\theta$ diagram for the stations in Fig. 5.

Bottom Water, North Atlantic Deep Water, and Antarctic Intermediate Water show up in the τ distribution. The last two are easily identified. Antarctic Bottom Water appears as the layer of minimum τ at the bottom in the southern hemisphere.

The superimposed contours of τ and σ_θ in Fig. 10 parallel each other only in the upper 1000 m and throughout the depth in the latitudinal band $35^\circ\text{N} \leq \varphi \leq 40^\circ\text{N}$. Again a θS relationship is indicated, and one can see this in the θS

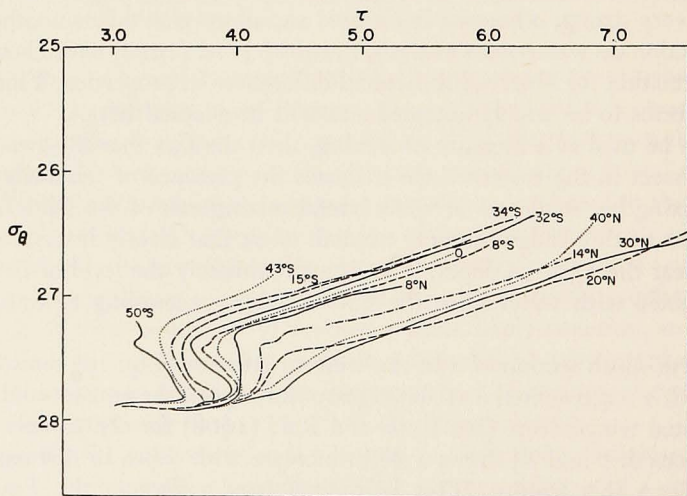


Figure 8. The $\tau\sigma_\theta$ diagram for the stations in Fig. 6.

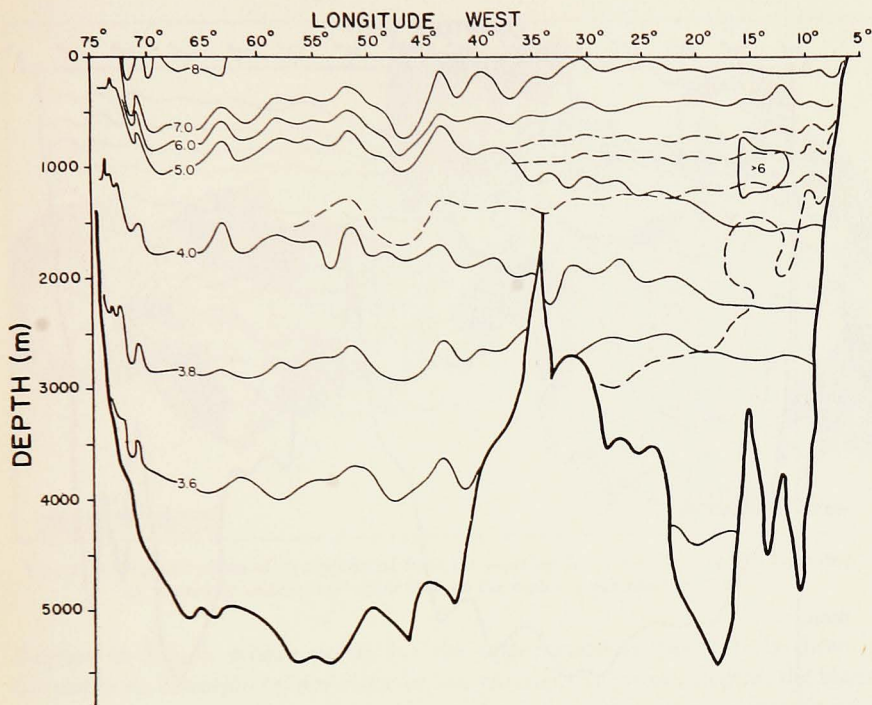


Figure 9. A vertical section of τ along 36°N in the Atlantic. Dashed curves are contours of $\sigma_\theta = \text{const}$, which intersect curves of $\tau = \text{const}$. Where no dashed curves are drawn, the two sets of curves are approximately parallel.

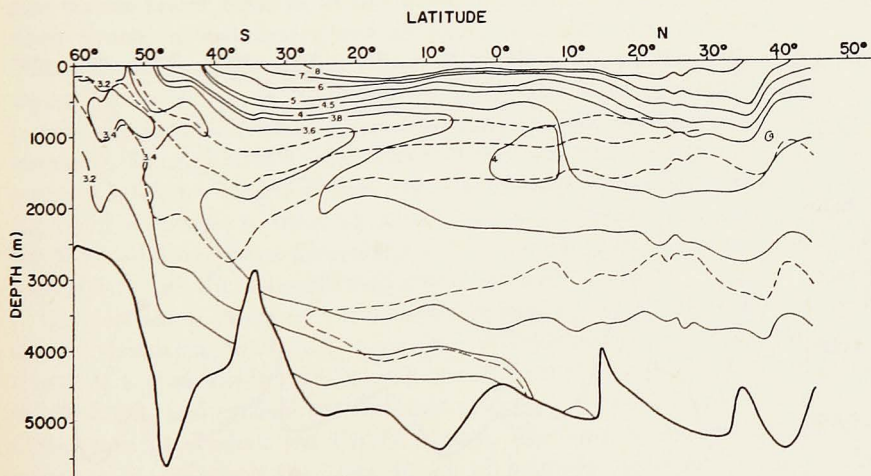


Figure 10. A meridional section of τ from station data in the western Atlantic. Dashed curves are contours of $\sigma_\theta = \text{const}$, which intersect curves of $\tau = \text{const}$. Where no dashed curves are drawn, the two sets of curves are approximately parallel.

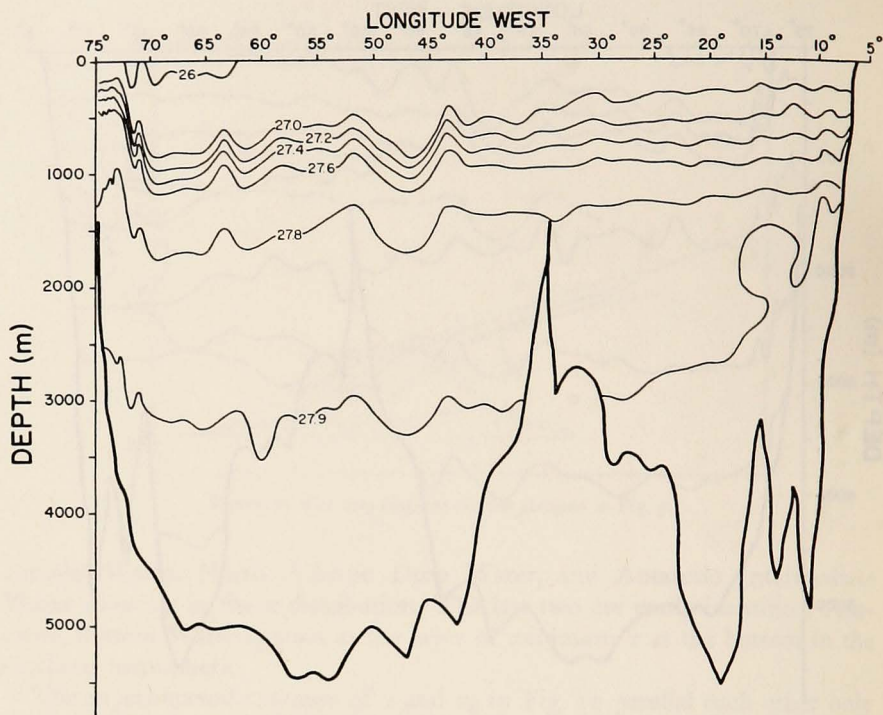


Figure 11. A vertical section of σ_θ along 36°N in the Atlantic.

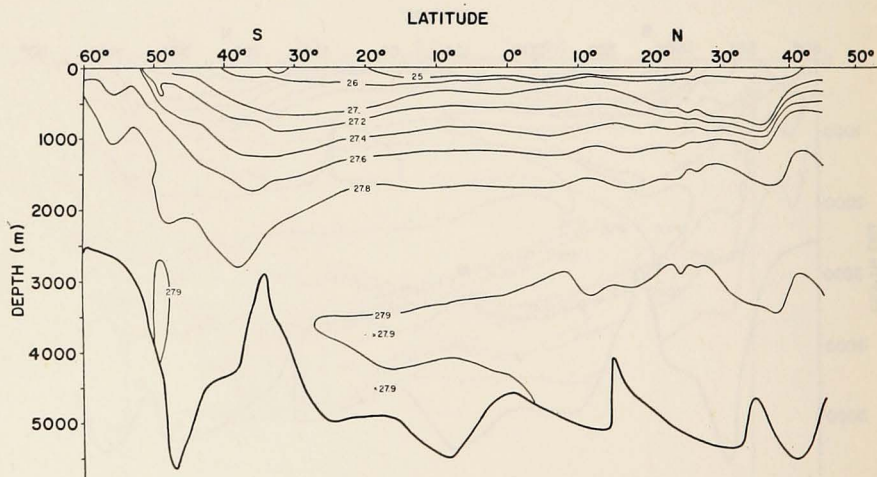


Figure 12. A meridional section of σ_θ for the data in Fig. 10. The mild reversal of σ_θ at great depth indicates instability according to σ_θ .

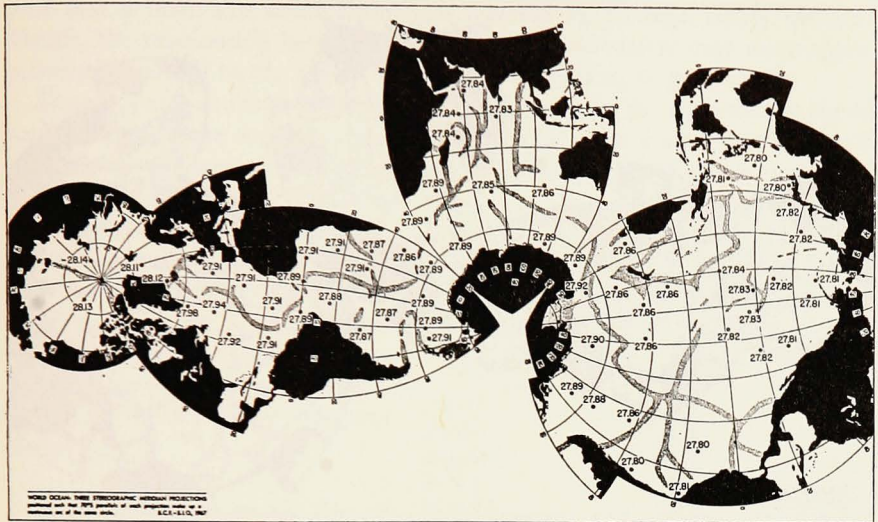


Figure 13. Abyssal values of σ_θ reproduced from the paper by Lynn and Reid (1968). The values of σ_θ are nearly uniform and show little of the variation exhibited by S and θ .

diagram in Fig. 6, where curves for the upper 1000 m (particularly those in the southern hemisphere) are more or less parallel. At greater depths, the intersection of τ and σ_θ contours provides evidence that these two quantities have distributions that are determined by different physical processes. If the intersection of isopleths is interpreted as an indication of mixing, the suggestion is that waters below 1000 m in the western Atlantic Basin are subject to relatively strong vertical mixing and moderate or weak horizontal mixing.

A different type of display is shown in Figs. 13, 14, and 15. Fig. 13 includes abyssal values of σ_θ , as calculated by Lynn and Reid. Except for the large (>28) values in the Arctic Ocean, the values of σ_θ do not vary much in abyssal waters. Lynn and Reid's calculations of σ_4 , potential density referred to the 4000-m level, are shown in Fig. 14; note that there is substantial variation in σ_4 , and it is possible to trace a gradual change of σ_4 from the source regions in the Weddell Sea and the Greenland Sea to other regions. Lynn and Reid have used σ_4 to trace the movement of abyssal waters.

Corresponding values of τ are shown in Fig. 15. Low values of τ occur in the source regions for abyssal waters (the Weddell Sea and the Greenland Sea). There is a gradual increase in τ in the Antarctic Ocean eastward from the Weddell Sea, and gradual increases are evident northward from the Antarctic Ocean into the Indian and Pacific oceans. The eastern Atlantic shows large values of τ , reflecting the large values of potential temperature there. The maximum value of τ in the western Atlantic coincides with the maximum potential temperature at about 45°N . Hence, τ exhibits many of the same

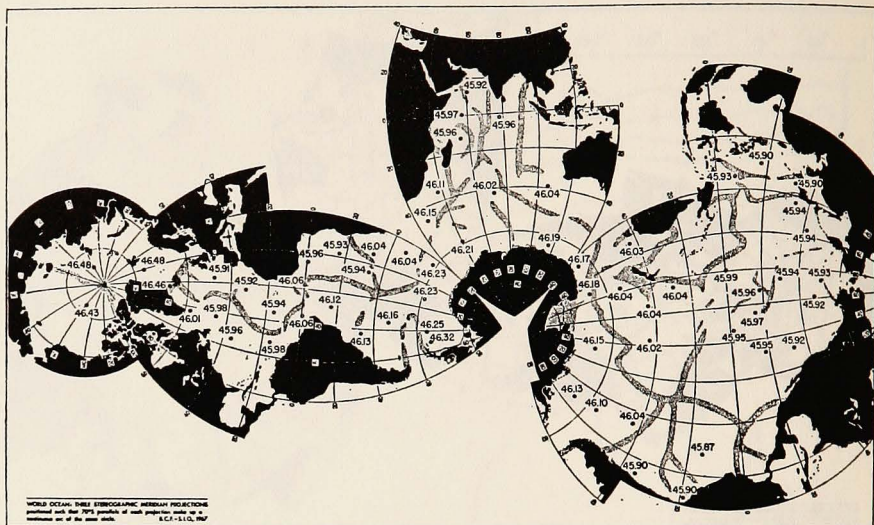


Figure 14. Abyssal values of σ_4 reproduced from the paper by Lynn and Reid (1968) for the same stations shown in Fig. 13. The distribution of σ_4 values shows sufficient structure to allow σ_4 to be used as a tracer for abyssal-water movement.

features as σ_4 . Potential density, on the other hand, is nearly uniform at great depth and does not correlate at all with σ_4 .

Stommel (1962) attributed the observed TS relationship of abyssal waters to a probable uniformity in τ . It appears from the present cursory study of the

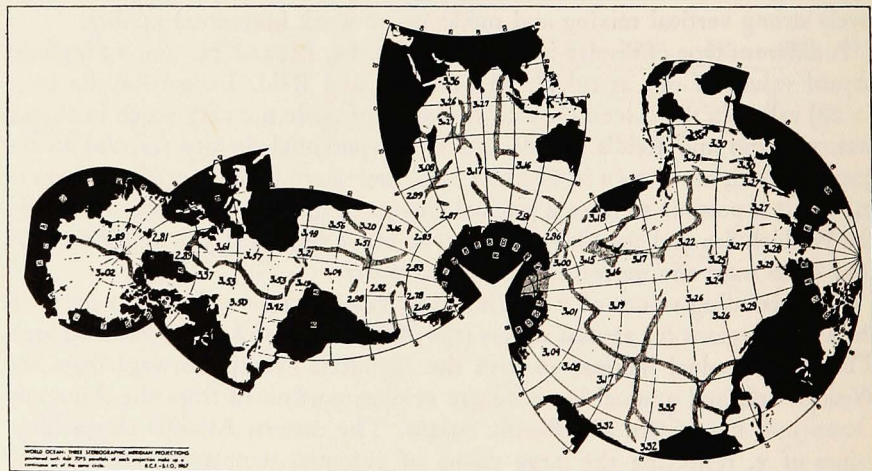


Figure 15. Abyssal values of τ for the station data in Figs. 13 and 14. The correlation between τ and σ_4 is high, indicating that τ is as good a tracer as σ_4 .

data that τ maintains small differences whereas σ_θ becomes nearly uniform. Hence, the relationship between θ and S for abyssal waters may more appropriately be related to the approximate uniformity of σ_θ at great depth.

Since σ_4 , as calculated by Lynn and Reid, contains the dynamically significant portion of the density at great depth, the fact that τ correlates well with σ_4 whereas σ_θ does not indicates that, at great depth, τ rather than σ_θ is dynamically significant. This observation is particularly surprising, because σ_θ was chosen because of its dynamical significance so that τ could be looked upon as a dynamically passive tracer. An attempt to resolve this point is contained in the following two sections.

4. A Limitation on the Use of σ_θ for Dynamical Purposes.

Although potential density is defined so as to incorporate the dynamically significant parts of temperature and salinity, it cannot be used indiscriminately. One of the problems that can arise can be seen by looking at the stability of typical parcels of seawater at great depths.

For example, consider two elements of seawater with temperatures and salinities that are typical of abyssal water (pressure = 4000 db) in the North Atlantic. These are shown in Table I along with the calculated⁸ common value $\sigma = 45.93$. The potential temperatures are also shown, as are the potential densities (actually σ_θ). It is evident from this example that two samples of water that are neutrally stable with respect to each other would appear to have a different relative stability according to potential density. Sample I would appear to be heavier when, in fact, it is not. In general, one can expect this behavior; i.e., elements of water with the same density but with different salinities and temperatures will show different densities when referred to another level. This behavior is associated with the different salinities and temperatures of the two elements and would, of course, not be possible when either S or T is constant.

An even more instructive example is shown in Table II. Here sample II is denser than sample I by about 0.02 units in σ . However, σ_θ of sample I is 0.01 units larger than σ_θ of sample II. Hence, from the potential density, one would conclude incorrectly that sample I is more dense. The differences shown are small, of course, but they are typical of abyssal waters. The conclusion is,

Table I. Calculated properties of two samples of seawater at a pressure of 4000 db with the same density but with different temperatures and salinities.

	Sample I	Sample II
T (°C).....	2.30	2.09
S (‰).....	34.90	34.85
σ (g/L).....	45.93	45.93
θ (°C).....	1.95	1.74
σ_θ (g/L).....	27.92	27.89

8. The quantities σ , θ , and σ_θ were calculated with the formulae used at the Woods Hole Oceanographic Institution for these quantities. Density (or σ) is obtained by using Ekman's (1908) empirical formula. Potential temperature (θ) is calculated from the polynomial expression by Fofonoff and Froese (1958). Potential density (σ_θ) is derived from the Knudsen (1901) formula for σ_t , with θ replacing T .

therefore, that small differences in the salinities and temperatures of abyssal waters can lead to potential densities that yield incorrect information with regard to gravitational stability. In general, in a multicomponent system, potential density cannot be used as an unambiguous measure of the dynamical behavior of the system. Potential density can still be used for other purposes, but its use for the determination of stability must be made with caution, particularly when the differences that are involved are small.

Table II. Calculated properties of two samples of seawater at a pressure of 4000 db with different densities, temperatures, and salinities.

	Sample I	Sample II
$T(^{\circ}\text{C})$	2.21	1.89
$S(\text{‰})$	34.90	34.85
$\sigma(\text{g/L})$	45.94	45.97
$\theta(^{\circ}\text{C})$	1.86	1.55
$\sigma_{\theta}(\text{g/L})$	27.92	27.91

The use of a deeper reference level (Kawai 1966, Lynn and Reid 1968) gives a better measure of the stability of deep waters. Although the error in stability is thereby shifted upward to shallower layers, the in situ variations are large enough to provide a better qualitative picture of stability.

Since the significance of potential density is the basis for the derivation and interpretation of the τ distributions that have been presented, it is important for our purposes to determine the specific significance of σ_{θ} in abyssal waters. We shall make this determination by comparing stability as calculated from σ_{θ} and from in situ density.

5. *In situ Stability and Local Potential Density.* We have seen that the use of potential density can lead to errors in the determination of gravitational stability of abyssal waters. It is well known (Hesselberg and Sverdrup 1914) that gravitational stability to infinitesimal disturbances can be determined by subtracting the in situ adiabatic density gradient from the observed density gradient. The resulting expression for gravitational stability is

$$E = - \left[\left(\frac{g}{\rho} \frac{\partial \rho}{\partial z} \right)_{\text{observed}} - \left(\frac{g}{\rho} \frac{\partial \rho}{\partial z} \right)_{\text{adiabatic}} \right], \quad (16)$$

$$= - \frac{g}{\rho} \left\{ \frac{\partial \rho}{\partial T} \left[\left(\frac{\partial T}{\partial z} \right)_{\text{observed}} + g \rho \frac{\partial T}{\partial p} \right] + \frac{\partial \rho}{\partial s} \left(\frac{\partial s}{\partial z} \right)_{\text{observed}} \right\},$$

where hydrostatic balance has been used to evaluate the adiabatic temperature gradient,

$$\left(\frac{\partial T}{\partial z} \right)_{\text{adiabatic}} = \frac{\partial T}{\partial p} \frac{\partial p}{\partial z} = -g \rho \frac{\partial T}{\partial p}.$$

With z increasing upward, the water is gravitationally stable for $E > 0$: z is measured positive upward in (16).

Table III. Computed quantities for hydrographic data from CRAWFORD Station 127, 4 April 1957, Lat. $15^{\circ}45'S$, Long. $30^{\circ}59'W$. In the last two columns, (k) means $\times 10^k$.

Depth	T ($^{\circ}C$)	θ ($^{\circ}C$)	S (‰)	σ_{θ} (g/L)	τ (g/L)	σ_l (g/L)	In situ stability (sec^{-2})	σ_{θ} stability (sec^{-2})
1	27.24	27.24	37.106	24.248	9.937	24.248		
70	27.13	27.11	37.115	24.296	9.928	24.296	0.660(-5)	0.662(-5)
95	24.90	24.88	37.084	24.973	9.511	24.973	0.260(-3)	0.259(-3)
190	21.40	21.36	36.746	25.741	8.561	25.741	0.779(-4)	0.771(-4)
285	13.72	13.68	35.328	26.526	5.929	26.542	0.824(-4)	0.788(-4)
380	10.00	9.95	34.859	26.869	4.966	26.925	0.371(-4)	0.344(-4)
475	7.54	7.49	34.621	27.072	4.404	27.155	0.228(-4)	0.203(-4)
570	5.82	5.77	34.473	27.187	4.026	27.296	0.138(-4)	0.116(-4)
765	4.02	3.96	34.387	27.325	3.671	27.470	0.828(-5)	0.673(-5)
955	3.57	3.50	34.464	27.432	3.633	27.591	0.588(-5)	0.539(-5)
1150	3.70	3.61	45.658	27.576	3.764	27.727	0.673(-5)	0.700(-5)
1345	4.01	3.90	34.850	27.699	3.936	27.839	0.542(-5)	0.602(-5)
1540	3.83	3.70	34.931	27.783	3.948	27.930	0.442(-5)	0.413(-5)
1740	3.46	3.32	34.935	27.825	3.874	27.989	0.274(-5)	0.196(-5)
1910	3.11	2.96	34.928	27.853	3.796	28.034	0.258(-5)	0.159(-5)
2105	2.97	2.80	34.916	27.858	3.756	28.049	0.650(-6)	0.227(-6)
2300	2.87	2.69	34.912	27.865	3.730	28.064	0.697(-6)	0.355(-6)
2585	2.75	2.54	34.909	27.875	3.697	28.084	0.669(-6)	0.348(-6)
2875	2.69	2.45	34.909	27.883	3.679	28.098	0.463(-6)	0.251(-6)
3170	2.64	2.37	34.907	27.888	3.660	28.111	0.381(-6)	0.170(-6)
3465	2.52	2.22	34.910	27.903	3.630	28.139	0.903(-6)	0.481(-6)
3755	2.27	1.94	34.900	27.918	3.565	28.181	0.135(-5)	0.470(-6)
4050	1.81	1.46	34.842	27.907	3.430	28.225	0.138(-5)	-0.325(-6)
4345	1.13	0.77	34.762	27.890	3.238	28.291	0.211(-5)	-0.560(-6)
4740	0.41	0.03	34.691	27.876	3.041	28.353	0.198(-5)	-0.347(-6)

Values of E for actual station data can be calculated numerically by using ordinary centered differences between levels. Comparison of in situ stability and stability according to σ_{θ} is shown in Tables III-V for data taken from stations in the South Atlantic, the North Atlantic, and the Mediterranean, respectively. A characteristic feature of open-ocean stations (Tables III and IV) is that near the surface σ_{θ} stability is only slightly smaller than the in situ stability whereas for abyssal waters the in situ stability is substantially larger. Indeed, near the bottom, σ_{θ} indicates instability whereas calculations based on E show mild stability.⁹ In Table V, data taken from the Mediterranean during the winter overturning in 1969 show instability at various depths, using both methods. Because of the general homogeneity of the water with depth (see θ and S values in Table V), the σ_{θ} stability calculation differs only slightly from E , and it can be used to determine gravitational instability.

9. That σ_{θ} indicates instability for abyssal Atlantic water while E shows stability has been known for a long time (Schubert 1935). However, it is not a well-known fact, even though some workers (e.g., Lynn and Reid 1968) have emphasized it very strongly.

Table IV. Computed quantities for hydrographic data from CHAIN Station 63, 6 May 1959, Lat. $36^{\circ}15'N$, Long. $22^{\circ}08'W$. In the last two columns, (k) means $\times 10^k$.

Depth	T ($^{\circ}C$)	θ ($^{\circ}C$)	S (‰)	σ_{θ} (g/L)	τ (g/L)	σ_l (g/L)	In situ stability (sec^{-2})	σ_{θ} stability (sec^{-2})
1	16.93	16.93	36.318	26.559	7.434	26.559	0.333(-6)	0.337(-6)
50	16.96	16.95	36.327	26.561	7.448	26.561	0.304(-4)	0.301(-4)
100	15.95	15.93	36.221	26.719	7.181	26.719	0.144(-4)	0.140(-4)
150	15.09	15.07	36.061	26.792	6.878	26.798	0.136(-4)	0.131(-4)
200	14.41	14.38	35.955	26.861	6.663	26.869	0.134(-4)	0.128(-4)
300	13.24	13.20	35.807	26.995	6.330	27.008	0.870(-5)	0.814(-5)
400	12.43	12.37	35.704	27.081	6.101	27.100	0.706(-5)	0.642(-5)
500	11.74	11.67	35.616	27.148	5.906	27.176	0.948(-5)	0.857(-5)
600	10.93	10.86	35.538	27.238	5.703	27.274	0.886(-5)	0.817(-5)
700	10.42	10.33	35.526	27.324	5.606	27.369	0.121(-4)	0.115(-4)
800	10.01	9.91	35.587	27.444	5.593	27.494	0.103(-4)	0.953(-5)
900	9.57	9.46	35.617	27.544	5.545	27.604	0.109(-4)	0.994(-5)
1000	9.10	8.98	35.649	27.649	5.492	27.717	0.764(-5)	0.605(-5)
1200	7.81	7.68	35.552	27.776	5.173	27.880	0.540(-5)	0.294(-5)
1400	6.22	6.08	35.347	27.837	4.707	27.994	0.281(-5)	0.732(-6)
1648	4.88	4.73	35.162	27.856	4.307	28.069	0.200(-5)	0.294(-6)
1845	4.14	3.98	35.066	27.862	4.091	28.111	0.128(-5)	0.120(-6)
2140	3.50	3.32	34.987	27.866	3.906	28.152	0.137(-5)	0.647(-6)
2435	3.16	2.96	34.969	27.886	3.820	28.195	0.104(-5)	0.464(-6)
2731	2.93	2.70	34.958	27.900	3.760	28.227	0.687(-6)	0.250(-6)
3126	2.74	2.47	34.946	27.911	3.704	28.256	0.400(-6)	0.228(-7)
3523	2.61	2.30	34.929	27.912	3.658	28.274	0.305(-6)	-0.172(-8)
3921	2.53	2.18	34.916	27.912	3.624	28.287	0.323(-6)	0.363(-7)
4320	2.47	2.07	34.907	27.913	3.596	28.300	0.125(-6)	0.341(-8)
4719	2.48	2.03	34.903	27.913	3.585	28.305	0.262(-6)	-0.199(-8)
4819	2.50	2.03	34.901	27.911	3.585	28.294		

It was pointed out in § 4 that the reason for the difference in the two stability calculations is that seawater is a multicomponent fluid and that the various thermodynamic coefficients are functions of both temperature and salinity as well as pressure. The small differences in these coefficients for fluid elements with different T and S values give rise to changes in σ_{θ} that are sufficiently large to mask in situ density differences between the fluid elements. However, there is also a qualitative distinction between the two types of stability calculations. E is a measure of local stability to infinitesimal disturbances but it cannot determine whether a column of water is stable to finite amplitude disturbances. In particular, if some process is capable of carrying a layer of water from one depth where it is gravitationally stable to another depth, possibly over long horizontal distances, and if the layer does not mix appreciably with its surroundings during the course of the motion, the layer may arrive at a lower level where it would be gravitationally unstable. Since in situ stability calcula-

Table V. Computed quantities for hydrographic data from DISCOVERY Station 6749, 7 February 1969, Lat. $42^{\circ}04'N$, Long. $4^{\circ}51'E$. In the last two columns, (k) means $\times 10^k$.

Depth	T ($^{\circ}C$)	θ ($^{\circ}C$)	S ($^{\circ}/_{\infty}$)	σ_{θ} (g/L)	τ (g/L)	σ_l (g/L)	In situ stability (sec^{-2})	σ_{θ} stability (sec^{-2})
0	12.92	12.92	38.441	29.092	9.310	29.093		
96	12.90	12.89	38.441	29.100	9.303	29.110	0.702(-6)	0.698(-6)
193	12.91	12.88	38.442	29.101	9.304	29.101	0.164(-6)	0.162(-6)
289	12.93	12.89	38.444	29.102	9.307	29.102	0.327(-7)	0.352(-7)
386	12.96	12.90	38.444	29.099	9.310	29.099	-0.324(-6)	-0.315(-6)
435	12.96	12.90	38.447	29.102	9.313	29.103	0.758(-6)	0.749(-6)
483	12.96	12.89	38.444	29.102	9.308	29.102	-0.150(-6)	-0.165(-6)
532	12.96	12.88	38.442	29.102	9.304	29.102	0.123(-7)	-0.359(-8)
580	12.96	12.87	38.441	29.102	9.301	29.103	0.161(-6)	0.145(-6)
777	13.02	12.90	38.442	29.097	9.308	29.098	-0.277(-6)	-0.258(-6)
974	13.01	12.86	38.439	29.103	9.296	29.104	0.327(-6)	0.294(-6)
1130	12.99	12.82	38.426	29.102	9.271	29.105	0.547(-8)	-0.553(-7)
1226	12.98	12.79	38.421	29.103	9.260	29.107	0.190(-6)	0.130(-6)
1323	12.98	12.78	38.421	29.107	9.258	29.110	0.349(-6)	0.314(-6)
1420	12.99	12.77	38.418	29.105	9.252	29.109	-0.961(-7)	-0.113(-6)
1516	12.99	12.76	38.413	29.105	9.243	29.109	-0.194(-7)	-0.670(-7)
1613	12.99	12.74	38.411	29.107	9.237	29.111	0.214(-6)	0.168(-6)
1808	13.00	12.72	38.410	29.110	9.231	29.115	0.219(-6)	0.186(-6)
2002	13.03	12.72	38.408	29.109	9.228	29.115	-0.437(-7)	-0.478(-7)
2099	13.06	12.73	38.409	29.107	9.232	29.112	-0.244(-6)	-0.190(-6)
2195	13.07	12.72	38.409	29.109	9.231	29.114	0.154(-6)	0.132(-6)
2242	13.07	12.71	38.408	29.110	9.228	29.116	0.244(-6)	0.177(-6)

tions cannot determine the relative stability of widely separated waters, some other determination must be made.

Potential density provides one such determination. For example, if a layer of water that is stable according to E but is unstable according to σ_{θ} were to be displaced adiabatically toward the surface, it would become unstable at some higher level. In the absence of such a vertical displacement, the water is, of course, stable.

From a practical point of view, a comparison of the two stability calculations may provide significant information. At high latitudes, near-surface waters that sink and become abyssal water may stratify at deep levels in a manner other than that indicated by their respective densities at the points of origin. An indication of this type of behavior can be seen in the paper by Lynn and Reid (1968). Their fig. 4 shows that water flowing south over the Greenland-Iceland Ridge has a higher potential density than water flowing north from Antarctica. Yet, near the equator these two water masses stratify, with Antarctic water lying below Arctic water. Their fig. 10 shows that the in situ stability¹⁰ of the abyssal waters near the equator is the opposite of what one would expect by

10. Their σ_4 distribution provides an exact in situ stability at 4000 m.

Table VI. Values of A_{ij} for the polynomial expression for τ . (k) means 10^k .

j	$i =$	1	2	3
1.....		5.089907	0.1529522	-0.2653792(-2)
2.....		0.8424673	0.2309882(-1)	-0.8486828(-3)
3.....		0.6951154(-1)	-0.1173089(-2)	0.6613862(-4)
4.....		-0.1263383(-2)	-0.1542035(-4)	-0.2640413(-5)
5.....		0.2008858(-4)	-0.1205016(-4)	-0.9072095(-5)
6.....		-0.1178271(-3)	0.7019903(-6)	0.4057835(-5)
j	$i =$	4	5	6
1.....		0.9409070(-4)	-0.3334090(-5)	0.5986311(-7)
2.....		0.5136553(-4)	-0.3040085(-5)	0.7860879(-7)
3.....		-0.1241726(-5)	-0.7876663(-6)	0.4358532(-7)
4.....		-0.3038523(-5)	0.1563445(-6)	0.4513363(-8)
5.....		0.6932661(-6)	0.1004874(-6)	-0.4025061(-8)
6.....		0.1928200(-6)	-0.2404088(-7)	0.6693087(-9)

comparing the potential densities near the points of origin (even at great depth). It is important to note that this effect is not due to mixing alone. Potential density is a property of the water at the point of measurement, hence the effect of mixing processes that have occurred as the water moved from its point of origin is included in the determination of σ_θ . But an added contribution is provided by the different adjustments in density that water masses with different values of T and S make when moved adiabatically from one level to another. The implication of the foregoing discussion is that the densest waters are generated in the Greenland Sea but that the density adjustment of this water during sinking is such that it is lighter than Antarctic Bottom water where they meet; the Greenland Sea water therefore lies above the Antarctic Bottom water at great depth.

In order to obtain an overall view of gravitational stability for a vertical section one can, of course, plot values of E at observed points. However, the following alternative approach may be preferable. From the expression for E , one can write the dynamically significant vertical-density gradient as

$$\frac{\partial \sigma_l}{\partial z} \equiv 1000 \frac{\partial \rho_l}{\partial z} = -1000 \frac{\rho}{g} E, \quad (17)$$

where ρ_l is defined as the local potential density¹¹ and $\sigma_l \equiv 1000(\rho_l - 1)$. Using the measured value of ρ at the surface (or below the mixed layer, say at 100 m) as a boundary condition, one can integrate eq. (5) downward to obtain

$$\rho - \rho_{\text{surface}} = - \int_0^z \frac{g}{\rho} E dz,$$

or

11. ρ_l is, in fact, simply the vertically integrated in situ stability.

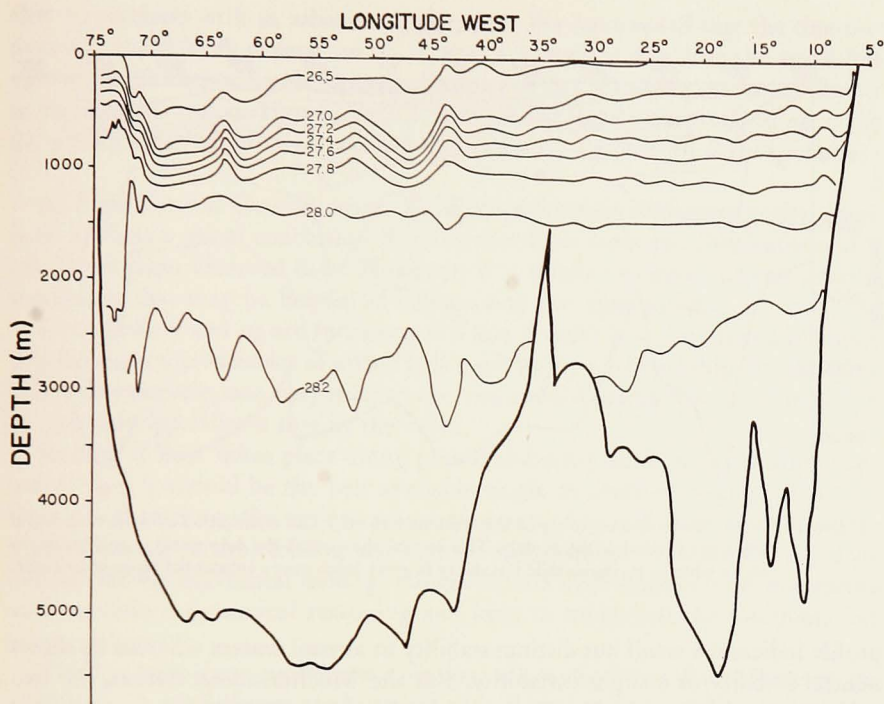


Figure 16. A vertical section of σ_l along 36°N in the Atlantic. The distribution of σ_l is meaningful along the vertical direction only. This section shows that the deep water is gravitationally more stable according to σ_l than according to σ_θ .

$$\sigma_l = \sigma_{\text{surface}} - 1000 \int_0^z \frac{g}{\rho} E dz. \quad (18)$$

[With actual station data, the integral is evaluated numerically. In the vertical sections of σ , shown later, the integral is calculated to an accuracy of $(\Delta z)^4$.] Here, σ_l corresponds to the dynamically significant value of the density; i.e., the adiabatic gradient at *each level* has been subtracted out in calculating E . The difference between σ_θ and σ_l is that in the σ_θ calculation the adiabatic adjustment is based on the values of T and S for the particular water element at z whereas for σ_l the adiabatic adjustment is based on the local properties of the water at each level about z . Essentially, σ_θ is associated with a Lagrangian type of displacement, σ_l with an Eulerian displacement. The vertical distribution of the local potential density provides an integral look at E for that location.

Values of σ_l are listed for three stations in Tables III–V, and vertical sections are plotted in Figs. 2–4. The graphs for the Atlantic stations show that σ_θ and σ_l have similar vertical distributions near the surface. However, the σ_l

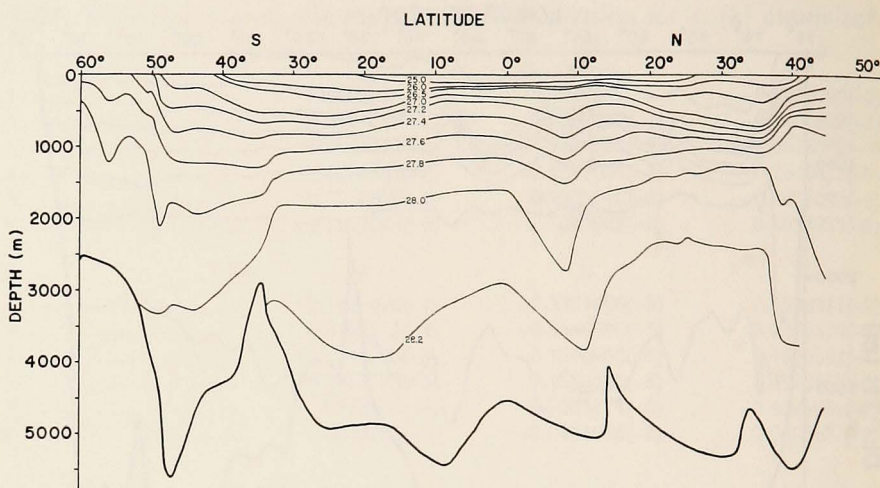


Figure 17. A meridional section of σ_l in the western Atlantic. The distribution of σ_l is meaningful along the vertical direction only. This section shows that the deep water is gravitationally stable whereas σ_θ shows mild instability at great depth over a substantial range of latitudes.

profile indicates a small but distinct stability in abyssal waters whereas σ_θ shows neutral stability or a slight instability. For the Mediterranean station, the two variables essentially coincide. However, in this case it is important to note that the maximum ranges of both σ_l and σ_θ are only 0.01 units; i.e., the column of water is nearly homogeneous and only the difference between maximum and minimum can be considered significant.

Two vertical sections of σ_l for the Atlantic Ocean are shown in Figs. 16 and 17. *The distributions of σ_l are meaningful only along each vertical*; i.e., one cannot compare horizontally adjacent values of σ_l because the local adiabatic gradients that have been subtracted out may differ. The graphs provide a picture of the in situ stability for each station, i.e., along the vertical at each location.

The corresponding sections of σ_θ are shown in Figs. 11 and 12. The western Atlantic section of σ_l indicates that the abyssal water is stable whereas σ_θ would indicate instability. For the purpose of determining gravitational stability for abyssal waters, the σ_θ section cannot be used whereas the σ_l section can be. The accuracy of the calculation of σ_l is limited only by the truncation error associated with the vertical spacing of station data. For determination of stability (and for that alone) σ_l is distinctly preferable to potential density irrespective of the level of reference chosen for σ_θ .

The results presented in this section provide useful information for the interpretation of the distribution of τ . As can be seen in Figs. 2 and 3, σ_θ does not correlate with σ_l at great depth whereas τ does. In Figs. 13–15 it is also evident

that τ correlates with σ_4 whereas σ_θ does not. We have noted that the thermodynamic coefficients depend on T , S , and p in such a way that the small but significant differences in the density distribution in deep water no longer appear in the σ_θ distribution. Hence, since τ was defined to be orthogonal to σ_θ in the θS plane, τ has acquired dynamical significance—by default, so to speak.

6. *Some General Considerations.* Since τ is a formally derived quantity, there is no obvious a priori conclusion that one can draw from the distributions of τ calculated from observed data. However, it is possible to make several general statements that may be helpful in interpreting the distributions.

First, since τ and σ_θ are functions of θ and S only, it is clear that a relationship between the variables of either pair must imply a relationship for the other pair. Alternatively, one may refer to the $\tau\sigma_\theta$ and θS planes to verify that a line in one plane specifies a line in the other.

Second, if flow takes place along potential-density surfaces, as is often supposed, then τ should be the best available single measure of mixing. Thus, in the vertical sections, the regions where contours of σ_θ and τ intersect are locations of strong vertical mixing and regions with parallel contours for τ and σ_θ indicate strong horizontal mixing. However, one must temper such statements with consistent dynamical reasoning and keep in mind that the interpretation is not unique.

Third, τ may show significant variations when the θ and S distributions are confusing. A preliminary study shows that this seems to be the case for the overturning of water in the northern Mediterranean during the winter of 1969. During overturning, the θ and S distributions show very small differences and σ_θ is essentially uniform. However, τ shows relatively significant variations. A more comprehensive analysis of this phenomenon is being pursued and will be reported later if the study proves to be fruitful.

Fourth, the fact that σ_θ is dynamically significant in the upper layers of the ocean but not in the deeper waters, combined with the fact that τ seems to acquire dynamical significance for deep water, means that some combination of σ_θ and τ with a weighting function of depth may be the most significant dynamical variable to choose. This point is complicated, because even the present superficial treatment of some observed data shows that σ_θ can be dynamically significant over only a shallow depth in one location but over almost the entire depth at another. That may mean that a single function of τ and σ_θ (or of θ and S) may not serve the purpose.

Fifth, at least three recent investigators (Kawai 1964, Lynn and Reid 1968) have proposed different reference surfaces for potential density as a means of studying the stability of deep waters and for tracing abyssal waters. The density referred to deeper layers gives a good picture of the stability in a thin horizontal layer. The use of σ_t gives a good picture of the stability along the local vertical plane. These two variables complement each other in usefulness.

Acknowledgments. I wish to thank J. L. Reid for sending me the world projection chart, in which values of τ are shown, and for offering his help with information about data sources. I am pleased to acknowledge several helpful discussions with Martin Mork and Henry Stommel. R. B. Montgomery, N. P. Fofonoff, R. O. Reid, and Maurice Rattray made useful suggestions after reading the original manuscript. The National Science Foundation supported this research with Grant GA 11410.

Data Sources. For the 36°N Atlantic section, the data are from the CHAIN 7 cruise as published in Fuglister's (1960) Atlas. Most of the data for the north-south section in the western Atlantic are also from Fuglister's Atlas. The station data south of 32°S are from DISCOVERY II stations 671, 673, 675, and from ELTANIN cruises 7-15 (Jacobs 1965). The abyssal data sources are in the paper Lynn and Reid (1968).

REFERENCES

- EKMAN, V. W.
1908. Die Zusammendrückbarkeit des Meereswassers. Publ. Circ. Explor. Mer, 43: 1-47.
- FOFONOFF, N. P., and C. FROESE
1958. Program for oceanographic computations and data processing on the electronic digital computer ALWAC III-E. PSW-1 Programs for properties of seawater. Ms. Rep. Ser. No. 27, Fish. Res. Bd. Can., Pac. Oceanog. Group. Nanaimo, B. C. (Unpublished manuscript).
- FUGLISTER, F. C.
1960. Atlantic Ocean atlas of temperature and salinity profiles and data from the International Geophysical Year of 1957-58. Woods Hole oceanogr. Inst., Atlas Ser., 1; 209 pp.
- HELLAND-HANSEN, BJØRN
1916. Nogen hydrografiske metoder. Skand. Naturfosker møte, Kristiana (Oslo).
- HESSELBERG, TH., and H. U. SVERDRUP
1914 or 1915. Die Stabilitätsverhältnisse des Seewassers bei vertikalen Verschiebungen. Bergens Mus. Aarb., 15: 1-16.
- JACOBS, S. S.
1965. Physical and chemical oceanographic observations in the southern oceans. USNS ELTANIN Cruises 7-15. Lamont geol. Observ., Tech. Rep. No. 1-cu-1-65; 321 pp.
- KAWAI, H.
1966. A generalized potential vorticity in the ocean. Spec. Contr. geophys. Inst., Kyoto Univ., 6: 69-93.
- KNUDSEN, MARTIN
1901. Hydrographical Tables. G.E.C. Gad, Copenhagen; Williams and Norgate, London.
- LYNN, R. J., and J. L. REID
1968. Characteristics and circulation of deep and abyssal waters. Deep-sea Res., 15: 577-598.

SCHUBERT, O. VON

1935. Die Stabilitätsverhältnisse im atlantischen Ozean. *Wiss. Ergebn. dtsh. atlant. Exped. 'Meteor', 1925-1927, 6 (2) (1): 54 pp.*

STOMMEL, HENRY

1962. On the cause of the temperature-salinity curve in the ocean. *Nat. Acad. Sci., 48: 764-766.*

SVERDRUP, H. U., M. W. JOHNSON, and R. H. FLEMING

1942. *The Oceans: their physics, chemistry and general biology.* Prentice-Hall, New York. 1087 pp.

WORTHINGTON, L. V., and W. R. WRIGHT

1970. North Atlantic Ocean atlas of potential temperature and salinity in the deep water including temperature, salinity and oxygen profiles from the Erika Dan cruise of 1962. Woods Hole oceanogr. Inst., Atlas Ser., 2.

WÜST, GEORG

1933. Das Bodenwasser und die Gliederung der atlantischen Tiefsee. *Wiss. Ergebn. dtsh. atlant. Exped. 'Meteor', 1925-1927. 6 (1) (1); 106 pp.*